Monte Carlo simulation of magnetic properties in nanocrystalline-like systems

2003 J. Phys.: Condens. Matter 15 6331

(http://iopscience.iop.org/0953-8984/15/37/003)

INSTITUTE OF PHYSICS PUBLISHING JOURNAL OF PHYSICS: CONDENSED MATTER

J. Phys.: Condens. Matter **15** (2003) 6331–6344 PII: S0953-8984(03)58726-4

Monte Carlo simulation of magnetic properties in nanocrystalline-like systems

O Crisan[1,2], Y Labaye[1], L Berger[1] and J-M Grenèche[1]

[1] Laboratoire de Physique de l'Etat Condensé, UMR CNRS 6087, Université du Maine, 72085 Le Mans Cedex 9, France
[2] National Institute for Materials Physics, PO Box MG-7, 76900 Bucharest, Romania

Received 20 January 2003, in final form 8 August 2003
Published 8 September 2003
Online at stacks.iop.org/JPhysCM/15/6331

Abstract

Those nanocrystalline materials which consist of ferromagnetic nanograins embedded in a ferromagnetic matrix were modelled as a cubic lattice composed of a central sphere with strongly coupled spins surrounded by weakly coupled spins. The magnetic behaviour was studied by Monte Carlo simulation, especially the low temperature spin ordering and features exhibited in the temperature range between the Curie temperatures of the two phases. The magnetization and magnetic susceptibility are calculated as a function of temperature for different values of the interfacial exchange interactions. It is shown that the exchange coupling between matrix and nanograin influences the magnetic properties of the nanograin, the matrix and the interfacial regions differently. The magnetic behaviour of different regions has been explained in terms of a polarization mechanism acting on the surface and in the core, leading to magnetic correlation between the spins. Such features are quite consistent with the experimental results obtained on nanocrystalline alloys.

(Some figures in this article are in colour only in the electronic version)

1. Introduction

The magnetic properties of nanocrystalline materials have been intensively studied, both experimentally [1–6] and theoretically [7–10], mainly due to their potential technological applications and their two-phase behaviour, respectively. Nanocrystalline alloys, like Finemet or Nanoperm, obtained by the annealing of amorphous precursors consist of nanograins dispersed within a ferromagnetic amorphous matrix. A key issue for understanding the magnetic macroscopic properties, such as magnetization or susceptibility, would be to investigate the contributions arising both from the nanograins and from the amorphous residual matrix, but also to elucidate the role played by the nanograin surface and the interfacial zone between the nanograins and the matrix. ^{57}Mössbauer spectroscopy studies of Finemet-type [2] and Nanoperm-type [3–6] nanocrystalline alloys provide evidence for an interfacial

zone between the nanograins and the amorphous residual matrix. This interface features a disordered atomic structure and spin-glass-like behaviour and has a chemical composition which differs strongly from those of both the nanograin and the matrix [6]. In addition, contrary to the low-temperature case where both intergranular and nanocrystalline grains behave as strongly coupled ferromagnets, the high temperature magnetic behaviour, i.e. above the Curie temperature of the amorphous matrix, is strongly dependent on the crystalline volume fraction. Superparamagnetic grains are observed for low crystalline fractions while penetrating fields originating from grains, tend to polarize the amorphous matrix for high crystalline fractions, preventing a purely paramagnetic state for the amorphous matrix [11–13].

Another key issue in understanding the magnetic properties of such systems is related to the surface and finite-size effects. Both effects have a stronger influence on the magnetic properties of the assemblies of nanograins, either isolated or interacting, as the size of the nanograins decreases. Several theoretical studies of the magnetic behaviour of oxide nanoparticles have been reported [7–10]. It has been shown that broken exchange bonds at the nanoparticles' surface, resulting in lower coordination compared to the bulk, give rise to a surface spin disorder and hence increased anisotropy [7]. The influence of the competition between bulk and surface energies resulting in finite-size effects on the magnetic behaviour of oxide nanoparticles have also been shown [7, 8]. The method of Monte Carlo simulation of low-temperature spin ordering has been employed for studying the surface and finite-size effects in oxide nanoparticles [9, 10]. Nevertheless, no theoretical studies on the magnetic properties of nanocrystalline soft magnetic alloys by Monte Carlo simulation have yet been reported, to our knowledge. Unlike micromagnetic [14, 15], or molecular field calculations [16], the Monte Carlo simulations take into account the atomic structure of the lattice and the short-range nature of the exchange interactions.

In the following, we present an approach, based on Monte Carlo simulation using a classical Metropolis algorithm, to model the magnetic properties of one ferromagnetic nanograin immersed in a ferromagnetic matrix. Different contributions to the total magnetization, arising from the core and surface of the nanograin, as well as from the interface between the nanograin and the matrix and from the matrix itself, will be shown. Moreover, the influence of the magnetic exchange coupling between the atoms in the surface and interface on the overall magnetization, as well as the magnetization of different regions, will be emphasized first and then the interfacial anisotropy will be discussed in conjunction with the occurrence of the canted interface layer.

It is important to emphasize that the structural and microstructural complexity of the nanocrystalline alloys prevents a simple structural model from being proposed. However, the present study aims only to show some phenomena usually observed on nanocrystalline alloys, especially those related to magnetic coupling between the two phases above the lowest Curie temperature [2]. Neither the chemical composition, nor the disordered structure of the amorphous phase are taken into account in the present cubic model. The magnetic parameters are chosen with values which differ from those characteristic of nanocrystalline alloys, but allowing some interesting features to be detailed [17].

2. Framework

Our starting model consists of a spherical nanograin embedded in a matrix of cubic shape. This cubic box contains 15^3 sites on a simple cubic lattice, i.e. each i site has 6 nearest neighbours. To each cubic lattice site we assign a classical spin S_i which interacts with its j nearest neighbours via an exchange coupling constant J_{ij}. Inside this box, we define a sphere of radius R (in units of the interatomic structure). The sites belonging to the sphere (nanograin) are denoted as A sites,

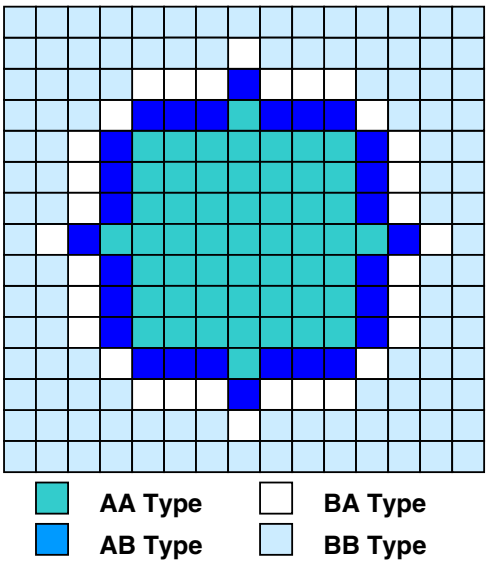

Figure 1. Middle plane of the 15^3 cubic box showing different regions: AA—nanograin; BB—matrix; AB—nanograin surface and BA—matrix–nanograin interface.

while the others, belonging to the matrix, are denoted as B sites. Moreover, we define two non-equivalent atomic layers at the nanograin surface: the first one consists of A sites having at least one first-nearest-neighbour of B type and denoted AB and the other consists of B sites having at least one first-nearest-neighbour of A type, denoted BA, as is shown in figure 1. These two atomic shells represent the nanograin surface and the matrix–nanograin interface, respectively, featuring magnetic behaviours different from that of the bulk (AA and BB regions). Taking into account the broken symmetry (lower coordination) for the sites in the surface, which leads to a distribution of magnetization over the whole system, one has to consider $J_{\mathrm{AA}} \neq J_{\mathrm{BB}} \neq J_{\mathrm{AB}}$ (for reasons of symmetry $J_{\mathrm{AB}} = J_{\mathrm{BA}}$). The macroscopic thermodynamic properties, such as the temperature dependence of magnetization, specific heat and magnetic susceptibility for our system, are obtained from a Heisenberg-type Hamiltonian which contains several terms corresponding to different energy contributions: exchange, anisotropy, magnetostatic, magnetoelastic, dipolar and thermal energy. In the present study, we only consider the first two prevailing energy contributions: the Hamiltonian defined at a given site i is thus

$$H_i = -\sum_{j \in V} J_{ij} \vec{S}_i \cdot \vec{S}_j - K_V (\vec{S}_{i,V} \cdot \hat{y})^2 - K_S (\vec{S}_{i,S} \cdot \hat{n})^2. \tag{1}$$

V is the nearest neighbourhood of site i, J_{ij} are the exchange coupling constants, S_i and S_j are the spins corresponding to the i and j sites, K_i is the site-dependent anisotropy constant ($K_i = K_S$ for AB sites and $K_i = K_V$ elsewhere) and θ_i is the angle between the easy axis and spin direction at each site, respectively.

For our simulations, we have chosen a system composed of one ferromagnetic nanograin, consisting of strongly coupled spins, embedded in a ferromagnetic environment with weakly coupled spins, typical of an amorphous residual matrix in a nanocrystalline soft magnetic alloy. The size of the cubic box was chosen to be 15^3 (3375 sites) and the grain had different radii, ranging from 4 ($N \approx 268$ sites) to 7 ($N \approx 1436$ sites). Those values correspond to an atomic crystalline fraction of 7 and 40%, respectively. The exchange coupling constants considered for calculations were $J_{\mathrm{AA}} = 3$ (inside the nanograin) and $J_{\mathrm{BB}} = 1/2$ (inside the matrix), a choice

consistent with two phases exhibiting significantly different Curie temperatures. The high ratio J_{AA}/J_{BB} thus allows us to separate clearly the two phases because the magnetic behaviour is worth discussing for a temperatures range between the two Curie temperatures. The exchange coupling constant between the nanograin and the matrix J_{AB} ranges from 0.01 to 50. It is obvious that one expects $J_{AA} > J_{AB} > J_{BB}$ in nanocrystalline alloys. Nevertheless, J_{AB} values over a rather large range were systematically considered to have a deep insight into the coupling exchange between the magnetic nanograin and matrix. It is important to emphasize that this model can be extended to different systems, including both strongly coupled magnetic and uncoupled systems such as exchange spring magnets (α-Fe/$Nd_2Fe_{14}B$), magnetic multilayers or magnetic nanoparticles dispersed into a diamagnetic or magnetic matrix. In addition, the present simple model is built on an assembly of magnetic moments, assumed to be the same in both grain and matrix, with one single interaction exchange value.

The calculations were performed using periodic boundary conditions. In order to obtain accurate magnetic data, one has to consider all of the above contributions to the Hamiltonian. In our case, the magnetic exchange interaction is considered only over the nearest neighbourhood and makes the strongest contribution to the energy. We have neglected the dipolar term in order to clarify the influence of the exchange coupling on the magnetic behaviour of each region. Moreover, the anisotropy is considered uniaxial along the y axis and equal for all sites, $K_V = 0.3$, while surface anisotropy was considered radial to the surface and equal to $K_S = 3.0$. The corresponding sites are located near the interface, i.e. two layers: one layer from the crystalline grain and one layer belonging to the matrix. Since no values of interface anisotropy can be found in the literature, to our knowledge, one can suggest the interface anisotropy is slightly larger than the bulk magnetocrystalline anisotropy but lower than the surface anisotropy, which is of the order of 0.01–1 mJ m^{-2} and 1–10 MJ m^{-2}, respectively, in cubic ferromagnets. We thus consider $K_S/K_V = 10$ in the present study.

The energy given in equation (1) is minimized by means of the Monte Carlo procedure [18]. During the simulation, Monte Carlo steps are used per spin with a random walk while angles are uniformly distributed over 4π. Starting with a random spin configuration at a temperature much higher than T_C, the energy is minimized using simulated annealing with a decreasing exponential law for temperature T^α with $\alpha = 0.96$ while thermodynamic quantities, such as magnetization, susceptibility and specific heat, can be derived as a function of temperature [18, 19]. By neglecting the dipolar term we thus use less CPU time for each computation. This gain thus allows a higher number of Monte Carlo steps (2×10^5 steps per spin and per temperature) to be taken in order to obtain better statistics for a more accurate estimation of thermodynamic quantities. Simulation of magnetic properties of the above described system considering different surface and volume anisotropies are then reported. The value of surface anisotropy was chosen to be extremely high to point out its effect on the magnetic arrangement at the interface between the nanograin and the matrix.

3. Results and discussions

We have represented, in figures 2 and 3, the temperature dependence of normalized magnetization of the 15^3 site cubic box, with different values of nanograin radius (comprised between 4 and 7) for several values of J_{AB} (exchange coupling between the matrix and the nanograin) ranging from 0.01 up to 50. All the curves show a two-phase behaviour, typical for nanocrystalline soft magnetic alloys. The two contributions which show distinct behaviour could unambiguously be attributed to the matrix and the nanograin, respectively. For low temperatures, the magnetization decreases sharply with increasing temperature, up to a

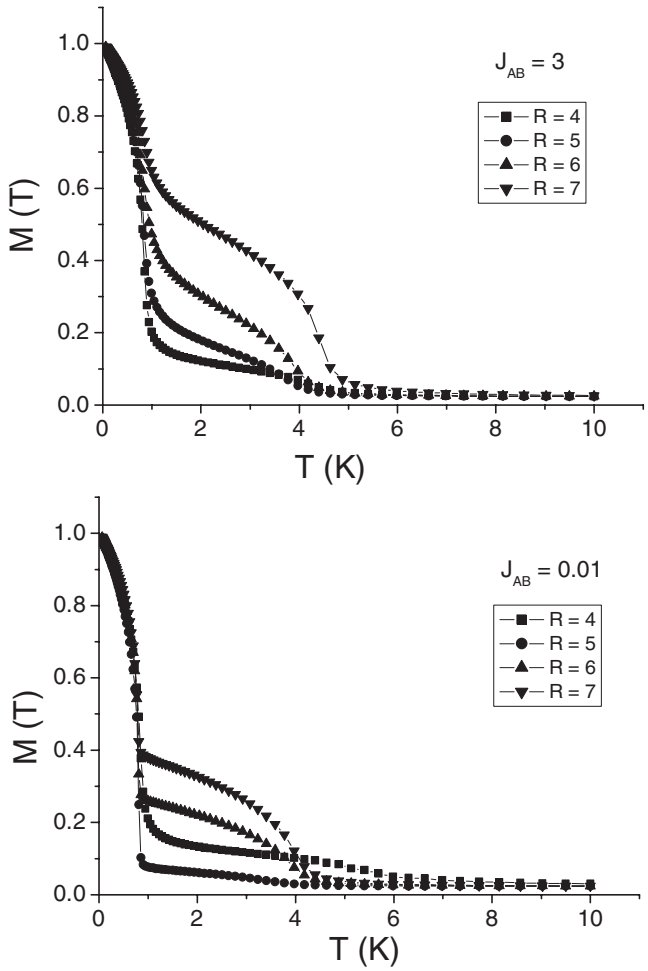

Figure 2. Temperature dependence of normalized magnetization of the system for a nanograin radius $R = 4$, 5, 6 and 7 and for a matrix–nanograin exchange coupling $J_{AB} = 0.01$ and 3.

temperature which is identified as the Curie temperature of the matrix (hereafter denoted T_C^M). Above T_C^M, the magnetization changes in slope and decreases slowly, typical for ferromagnetic materials, up to a temperature value identified as the Curie temperature of the nanograin (hereafter denoted T_C^N). It is worthwhile noting that the magnetization apparently does not vanish at temperatures above T_C^N. This is an illustration of the size effects acting on the magnetic state of the system. When one deals with finite-sized magnetic objects, finite-size effects are particularly severe in the critical region near the phase transition [20]. Consequently, the magnetic correlation established through exchange coupling between reversal spins does not completely disappear even at temperatures above T_C^N, where thermally activated magnetic fluctuations should prevent the local alignment of the spins. The magnetization curve with $J_{AB} = 0.01$ shows a very sharp transition between the matrix and the nanograin contributions, typical for a system with completely decoupled magnetic phases. With increasing J_{AB}, the transition between the two contributions becomes more and more smooth and one can observe that the exchange coupling in the surface influences the matrix and the nanograin differently.

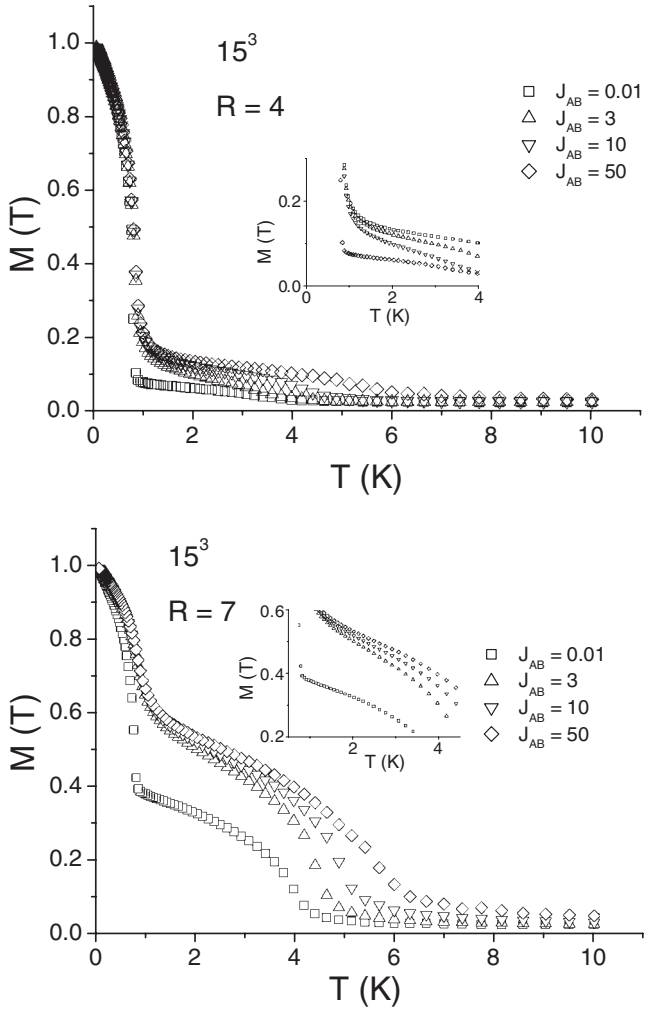

Figure 3. Temperature dependence of normalized magnetization of the system for a matrix–nanograin exchange coupling $J_{AB} = 0.01$, 3, 10 and 50 and for nanograin radius $R = 4$ and 7.

The magnetic susceptibility χ_V is calculated using the following relationship:

$$\chi_V = \frac{1}{V}\frac{\partial M}{\partial T} = \langle M^2 \rangle - \langle M \rangle^2 \tag{2}$$

where M corresponds to the total magnetization and $\langle\ \rangle$ means the thermal averaging over all configurations. The temperature dependence of the susceptibility, which is plotted on a logarithmic scale in figure 4, exhibits two peaks, corresponding to the contributions of both the matrix and the nanograin, in agreement with a two-phase behaviour. One can see that on increasing the coupling between the spins in the interface, the relative intensity of the peak corresponding to the matrix contribution decreases while the relative intensity of the peak corresponding to the nanograin contribution increases. The peaks occur at temperatures identified as T_C^M and T_C^N, respectively, which were estimated by numerical fitting of both the susceptibility and the total magnetization curves, the results being similar. For ferromagnetic

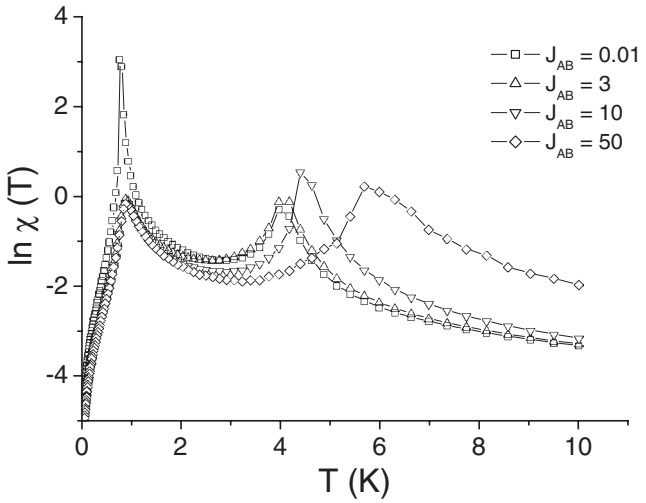

Figure 4. Temperature dependence of the susceptibility (in logarithmic scale) for the $R = 7$ nanograin immersed in the 15^3 cubic box for a matrix–nanograin exchange coupling $J_{AB} = 0.01$, 3, 10 and 50.

single-phase materials it is well known that the spontaneous magnetization decreases with temperature as follows:

$$M_s(T) = M_s(0)\left[1 - \frac{T}{T_C}\right]^{\beta} \tag{3}$$

where $M_s(0)$ is the saturation magnetization (magnetization at 0 K), T_C is the Curie temperature and β is the critical exponent. A typical value of 0.36 is expected for β in the case of ferromagnetic materials. Let us remark that the critical exponents describe the divergence of thermodynamic quantities, such as magnetization or susceptibility, at the critical points, such as Curie temperatures. Using the finite-size scaling theory, for a finite lattice with linear size L, the critical temperature is shifted compared to an infinite lattice by $L^{-1/\nu} \approx |T_C(L) - T_C|$, with L being the size of the system (in our case, the size of the cubic box) [20]. Consequently, it allows the critical temperature and critical exponents to be estimated.

Applying equation (3) to both the matrix and the nanograin, the magnetization curves were fitted by considering for both the matrix and the nanograin only the temperature regions not too far below T_C. This fitting allows a rough estimation of the T_C^M and T_C^N. We plot in figure 5 the Curie temperature for the nanograin versus the exchange coupling on the surface J_{AB} for nanograin sizes ranging from $R = 4$ to 7. The general trend for the T_C^N is almost the same whatever the nanograin size, i.e. a slight decrease up to an exchange coupling value $J_{AB} \approx 3$, which equals the exchange coupling constant J_{AA} of the nanograin itself, then an increase with a further increase of J_{AB}. Values of J_{AB} greater than three times the exchange coupling in the nanograin J_{AA} are unphysical, but they have been considered nevertheless to observe the general trend of the profiles. For our system, the region of interest is then for J_{AB} ranging between 0 and 10. For $J_{AB} = 0.01$, when the nanograin is almost completely decoupled from the matrix, the T_C of the nanograin (which means here all the A sites) is higher than the value expected if all the A sites would have the same exchange coupling constant. This could be due to the lack of magnetic correlation between the spins in the nanograin surface associated with a mechanism of depolarization of the nanograin core induced by the surface layer. By increasing the exchange coupling J_{AB} up to the J_{AA} value, the T_C^N decreases towards the minimum value

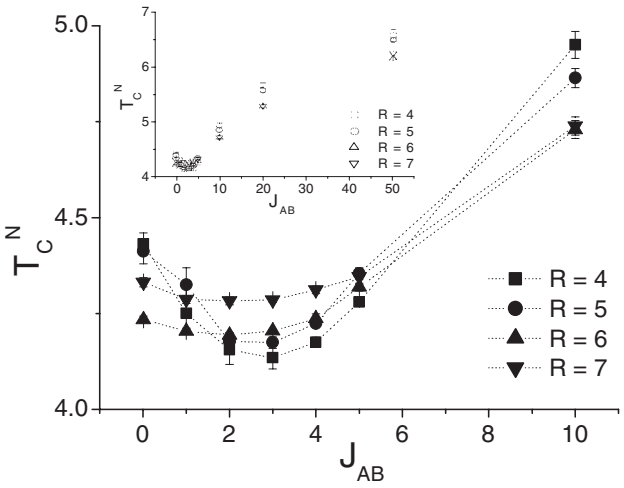

Figure 5. Curie temperature of the nanograin T_C^N versus exchange coupling J_{AB} for different nanograin radii. Inset: same curves plotted on an enlarged scale.

which corresponds to the situation where all the A spins are exchange-coupled with the same strength: in other words, when the surface layer does not influence the nanograin core. When the exchange coupling in the surface J_{AB} further increases, the T_C^N increases also. In this case the surface layer, being more strongly coupled than the core of the nanograin, induces stronger magnetic correlation between spins in the core, which indicates the polarization of the nanograin core by the surface layer.

The 'concavity' of the profile centred at $J_{AB} \approx J_{AA} = 3$ is more pronounced for small nanograin sizes and flattens as the nanograin radius increases. This is mainly due to the effect of the ratio between the number of sites in the surface and the number of sites in the core N_s/N_{core}. When the nanograin radius increases, the ratio N_s/N_{core} decreases, which leads to a smaller effect of polarization–depolarization of the core by the surface layer when varying the exchange coupling J_{AB}, and thus less pronounced concavity in the region centred at $J_{AB} \approx 3$. This behaviour is independent of the way of numerical fitting and is preserved for the T_C^N values obtained from the refinement of susceptibility curves.

In figure 6, the Curie temperature of the matrix T_C^M is plotted against the exchange coupling J_{AB} in the surface for different nanograin radii. All the curves show a sharp increase of T_C^M from the initial value corresponding to the almost decoupled system. Then the dependence reaches saturation for a maximum value for high values of J_{AB}. Nevertheless, the initial increase is sharper as the nanograin size increases. This increase of T_C^M could be explained as previously by a mechanism of polarization of the matrix by the interfacial layer between the matrix and the nanograin (BA region, i.e. the B atoms which have at least one A atom as first-nearest-neighbour). The increase in T_C^M is larger, for any values of J_{AB}, as the radius of the nanograin increases (meaning that there will be less atoms in the matrix and thus a higher ratio between the number of sites in the interface and the number of sites in the matrix N_{BA}/N_{BB}). It is also worthwhile to note that the curves reach saturation at higher values of J_{AB}, as the radius of the nanograin increases. For small nanograin radii (small N_{BA}/N_{BB} ratio) the polarization of the matrix by the stronger magnetically correlated interfacial region (BA region) is sudden, T_C^M sharply increases for $J_{AB} = 1$ and then the further increase in T_C^M, for higher values of J_{AB}, is almost negligible. In contrast, for larger nanograin radii (higher N_{BA}/N_{BB} ratio) the

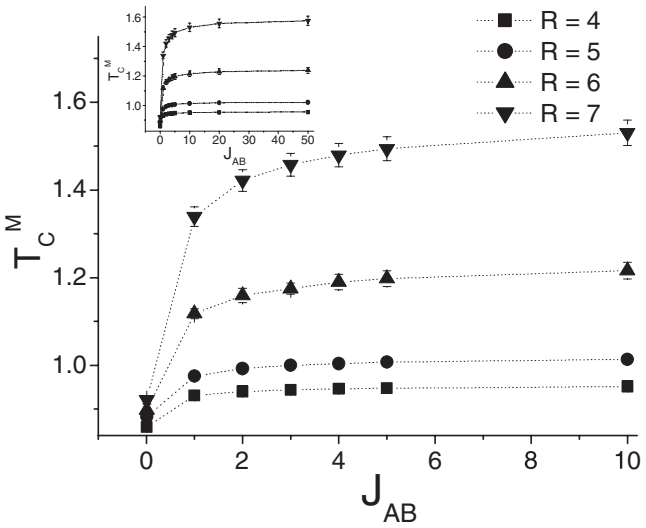

Figure 6. Curie temperature of the matrix T_C^M versus exchange coupling J_{AB} for different nanograin radii. Inset: same curves plotted on an enlarged scale.

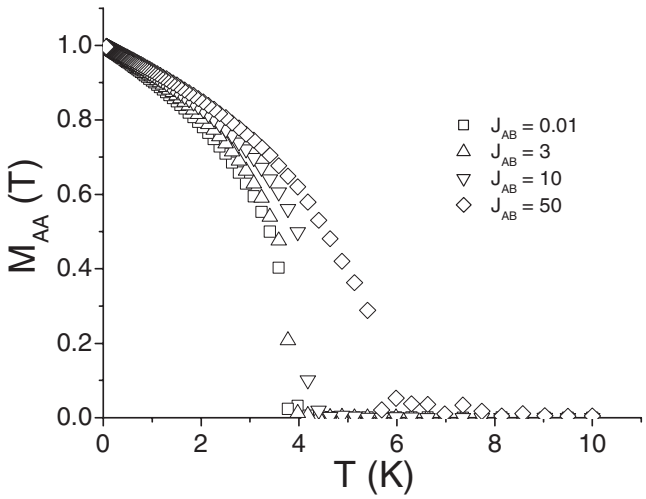

Figure 7. Temperature dependence of normalized magnetization of the nanograin core M_{AA} for a nanograin radius $R = 6$ and matrix–nanograin exchange coupling $J_{AB} = 0.01$, 3, 10 and 50.

polarization of the matrix by the BA region is gradual and the saturation is reached at higher values of J_{AB}.

4. Influence of exchange coupling

4.1. AA (ferromagnetic nanograin core)

Figure 7 shows the temperature dependence of the normalized magnetization for the nanograin core M_{AA} for the case $R = 6$ for different exchange couplings in the surface J_{AB}. The curves are typical for a ferromagnetic single-phase material with a decrease to zero at the T_C of the

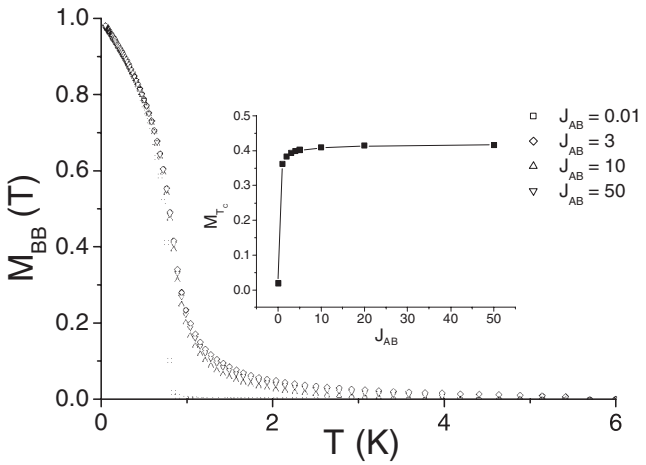

Figure 8. Temperature dependence of normalized magnetization of the matrix M_{BB} for a nanograin radius $R = 6$ and matrix–nanograin exchange coupling $J_{\mathrm{AB}} = 0.01$, 3, 10 and 50. Inset: values of M_{BB} corresponding to the T_{C} of the matrix for the almost decoupled system ($J_{\mathrm{AB}} = 0.01$) plotted versus J_{AB}.

nanograin core. The decrease is sharp for low values of J_{AB} and becomes sluggish as J_{AB} increases. With increasing the exchange coupling J_{AB} the T_{C} of the nanograin core follows the same trend as described before for the T_{C} of the whole nanograin ($T_{\mathrm{C}}^{\mathrm{N}}$) estimated by numerical fitting of the total magnetization curves (figure 3). Nevertheless, the increase of T_{C} of the nanograin, which is surprisingly high, is not consistent with experimental features. Indeed, the completely paramagnetic matrix does produce a decrease of both the Curie temperature and magnetization of the nanocrystalline grain through the presence of superparamagnetic fluctuations when the crystalline volumetric fraction is rather low, or does not influence the magnetic characteristics of the nanocrystalline grain, as observed experimentally (see [2] and references therein). The present results are thus not clarified. One finally observes for small nanograin radius that, at temperatures above T_{C}, the magnetization fluctuates. Note that, for higher nanograin radius, these fluctuations are less important because of the larger number of spins in the nanograin core. The presence of these fluctuations is thus attributed as a direct consequence of the finite nanograin size effects.

4.2. BB (ferromagnetic matrix)

The temperature dependence of the normalized magnetization due to the sites in the matrix M_{BB}, plotted in figure 8, is also typical for weakly ferromagnetic single-phase materials, with a sharp drop to zero at $T_{\mathrm{C}}^{\mathrm{M}}$ for the almost decoupled system ($J_{\mathrm{AB}} = 0.01$). With increasing J_{AB} the magnetic transition becomes smoother, illustrating the effect of the exchange coupling on the surface on the spins belonging to the matrix. In addition, one notes the increase of T_{C} which is correlated to that of the mutual exchange between the nanograin and the matrix, resulting from the core grain. Such an effect agrees with the increase of T_{C} which has been experimentally observed on nanocrystalline alloys [2, 13]. The differences between the magnetization values in the critical region decreases as the exchange coupling J_{AB} increases from 1 to 50. This difference can be seen if we plot (see the inset of figure 8) the different magnetization values corresponding to $T_{\mathrm{C}}^{\mathrm{M}}$ for the almost decoupled system ($J_{\mathrm{AB}} = 0.01$), $M_{T_{\mathrm{C}}}$ versus the exchange coupling J_{AB}. One can observe a behaviour almost similar to that of the $T_{\mathrm{C}}^{\mathrm{M}}$ as estimated from

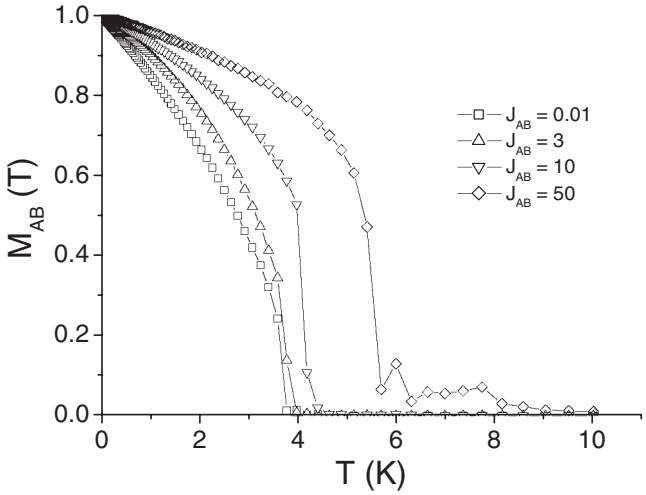

Figure 9. Temperature dependence of normalized magnetization of the nanograin surface M_{AB} for a nanograin radius $R = 6$ and matrix–nanograin exchange coupling $J_{AB} = 0.01$, 3, 10 and 50.

total magnetization fits. The dependence increases sharply from $J_{AB} = 0.01$ up to 1 and then reaches saturation for exchange couplings up to $J_{AB} = 50$. Taking into account that the spin moment equals 1 for every site, it means that, for $J_{AB} = 1$, up to 40% of the spins in the matrix are magnetically coupled at a temperature value (T_C) at which they should have been magnetically disordered in the absence of the coupling on the surface J_{AB}. This means that, when the nanograin and the matrix become magnetically coupled, several atomic layers in the matrix are being polarized by the exchange coupling in the surface. Further enhancement of the exchange coupling J_{AB} does not modify the amount of spins in the matrix being magnetically ordered by the interface layer.

4.3. AB (nanograin surface)

The temperature dependence of the normalized magnetization due to the A sites having at least one B site as first-nearest-neighbour (the surface of the nanograin) M_{AB}, plotted in figure 9, is almost similar for low exchange coupling constants J_{AB} and exhibits a different trend for high J_{AB} values, compared to the nanograin core. In fact, as J_{AB} increases, the magnetization curves show a more pronounced curvature, corresponding to a higher degree of magnetic correlation between the spins in the nanograin surface. As expected, the influence of increasing exchange coupling between the matrix and the nanograin is greater for the surface than for the nanograin core, at higher values of J_{AB}. As in the case of the nanograin core, fluctuations of the magnetization, due to size effects, are observed above the Curie temperature.

4.4. BA (matrix–nanograin interface)

The most important effect of the increasing exchange coupling J_{AB} is observed in the temperature dependence of magnetization for the sites in the interface layer between the nanograin and the matrix (B sites having at least one A site as first-nearest-neighbour) M_{BA}, plotted in figure 10. For $J_{AB} = 0.01$, the magnetization curve is typical for weak ferromagnets (i.e. with weakly coupled magnetic moments) as in the case of the matrix contribution M_{BB}. As the J_{AB} coupling increases, the behaviour changes drastically. At high J_{AB} values, the

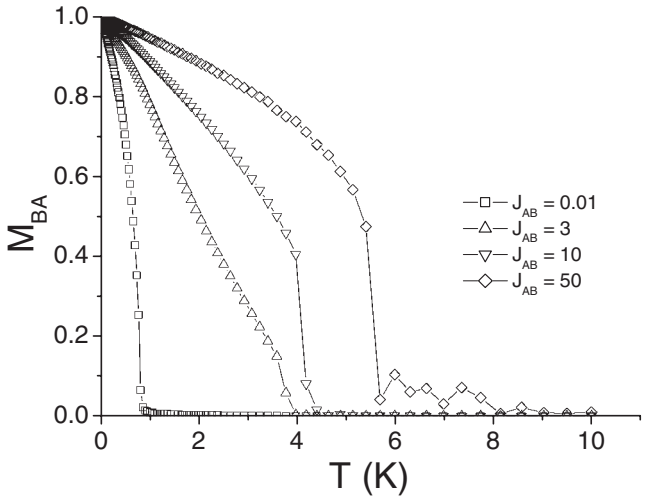

Figure 10. Temperature dependence of normalized magnetization of the matrix–nanograin interface M_{BA} for a nanograin radius $R = 6$ and matrix–nanograin exchange coupling $J_{AB} = 0.01$, 3, 10 and 50.

behaviour is typical for highly magnetically correlated single-phase materials. One can also observe that, contrary to the case of the matrix, for high J_{AB} values (>10) the system exhibits some magnetic fluctuations above T_C due to size effects, which become more important as the nanograin radius decreases, as in the case of the nanograin or surface.

When the surface anisotropy is considered, the previous results are rather similar; the two main differences are concerned, first, by the more intense polarization effect coming from the shape of the magnetization temperature dependence and, second, by the spin configuration which is schematically represented in figure 11. One clearly observes a non-collinear spin arrangement at the interface, due to the competition between surface anisotropy, which tends to orient the spins normal to the surface, and magnetocrystalline anisotropy, which tends to orient them along the *y* axis. It originates thus in a perturbed magnetic ordering of the interfacial shells of the nanograin, because the spins in the interface are exchange-coupled to neighbouring shells in the nanograin core and matrix. It is important to compare this spin-glass-like configuration in the interfacial regions to the 'throttled' structure—like in the case of a nanoparticle which results from the surface anisotropy competing with the bulk magnetocrystalline [21]. It is noteworthy to add that this spin-glass-like ground state has been suggested from in-field Mössbauer experiments performed on some soft magnetic nanocrystalline alloys [22].

5. Conclusions

The magnetic behaviour of a nanocrystalline alloy has been modelled by means of one ferromagnetic nanograin embedded in a ferromagnetic matrix, both with cubic symmetry environments. The low temperature spin ordering has been followed as a function of the magnetic interaction between the two phases, using Monte Carlo simulation, in addition to the different contributions to the total magnetization of the system, arising from the nanograin core, nanograin surface, interface between the nanograin and the matrix, and from the matrix itself. By fitting the temperature dependence of the total magnetization by means of a power law, we estimated the Curie temperatures corresponding to the nanograin and the matrix,

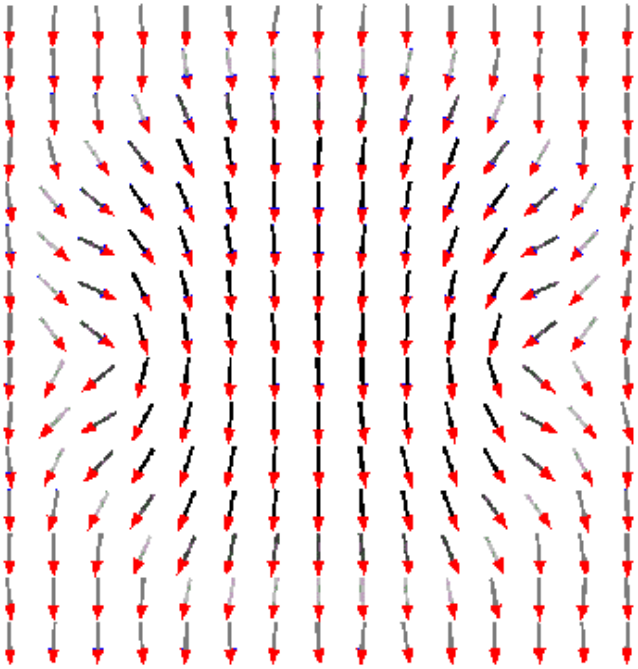

Figure 11. Spin configuration of the middle plane of the 15^3 cubic box containing the spherical nanograin, $R = 6$ and $K_S = 3.0$. The y axis corresponds to the vertical direction.

respectively. We have shown for the first time that, upon increasing the exchange coupling between the spins in the surface and interface, the magnetic behaviour of different regions of our system is governed by a spin polarization–depolarization mechanism which induces magnetic correlation between the spins. In addition, the strong exchange coupling in the surface originates a magnetic polarization inside the matrix which extends along at least two successive atomic layers. The exchange coupling between spins in the surface and interface influences differently each region of our system and this influence has been qualitatively evaluated and correlated with the ratio between the number of sites in the surface and number of sites in the nanograin core.

Acknowledgments

The authors would like to thank Professor J M D Coey (Dublin) for stimulating discussions during this work. The financial support of Region Pays de Loire for the Post-doctoral position of OC at LPECis gratefully acknowledged. The Monte Carlo simulation has been performed at the Lotus, a 70-processor, Beowulf class, home-made parallel computer at LPEC (web site: http://weblotus.univ-lemans.fr/w3lotus).

References

[1] Crisan O, Le Breton J M, Jianu A, Teillet J and Filoti G 1997 *J. Alloys Compounds* **262/263** 381
[2] Grenèche J-M, Miglierini M and Slawska-Waniewska A 2000 *Hyperfine Interact.* **126** 27
[3] Miglierini M and Grenèche J-M 1999 *Hyperfine Interact.* **120/121** 297
[4] Miglierini M and Grenèche J-M 1999 *Hyperfine Interact.* **122** 121

[5] Skorvanek J, Kovac J and Grenèche J-M 2000 *J. Phys.: Condens. Matter* **12** 9085
[6] Grenèche J-M and Slawska-Waniewska A 2000 *J. Magn. Magn. Mater.* **215/216** 264
[7] Kodama R H and Berkowitz A E 1999 *Phys. Rev.* B **59** 6321
[8] Kodama R H 1999 *J. Magn. Magn. Mater.* **200** 359
[9] Kachkachi H, Noguès M, Tronc E and Garanin D A 2000 *J. Magn. Magn. Mater.* **221** 158
[10] Kachkachi H, Ezzir A, Noguès M and Tronc E 2000 *Eur. Phys. J.* B **14** 681
[11] Hernando A and Kulik T 1994 *Phys. Rev.* B **49** 7064
[12] Suzuki I and Cadogan J M 1998 *Phys. Rev.* B **58** 2730
[13] Garitaonandia J S, Schmool D S and Barandiaran J M 1998 *Phys. Rev.* B **58** 12147
[14] Kronmüller H, Fischer R, Hertel R and Leineweber T 1997 *J. Magn. Magn. Mater.* **175** 177
[15] Kronmüller H, Fischer R, Bachmann M and Leineweber T 1999 *J. Magn. Magn. Mater.* **203** 12
[16] Fruchart O, Nozières J-P, Kevorkian B, Toussaint J-C, Givord D, Rousseaux F, Decanini D and Carcenac F 1998 *Phys. Rev.* B **57** 2596
[17] Crisan O, Labaye Y, Berger L and Grenèche J-M 2002 *J. Appl. Phys.* **91** 8727
[18] Binder K and Heermann D W 1992 *Monte Carlo Simulation in Statistical Physics* (Berlin: Springer)
[19] Kirkpatrick S, Gelatt C D Jr and Vecchi M P 1983 *Science* **220** 671
[20] Binder K 1976 *Phase Transitions and Critical Phenomena* vol 5B, ed C Domb and M S Green (New York: Academic)
[21] Labaye Y, Crisan O, Berger L, Grenèche J-M and Coey J M D 2002 *J. Appl. Phys.* **91** 8715
[22] Slawska-Waniewska A and Grenèche J-M 1997 *Phys. Rev.* B **56** R8491